ROYAL SOCIETY
OF CHEMISTRY

PAPER

Check for updates

Bioconversion of self-neutralized chemically depolymerized lignin streams into polyhydroxyalkanoates

Gordon L. W. Winkler,[a] Kai Gao, [iD] [b] Ethan M. Seng,[a] Charles N. Olmsted,[a] Rachel Rovinsky,[a] Deepak Kumar, [iD] [c] Blake A. Simmons, [iD] [bd] Hemant Choudhary [iD] *[be] and Erica L.-W. Majumder [iD] *[a]

Lignin is a chemically complex, diverse, and abundant plant polymer mainly composed of aromatic monomers. These aromatic monomers make lignin a potential source of aromatics and a viable substitute for petrochemically-derived aromatics. However, the structural recalcitrance of lignin requires harsh reagents from the chemical process and expensive catalysts for effective depolymerization. This chemical process often results in poor yields of chemical intermediate mixtures of varying bioavailability and/or toxicity. Furthermore, the cost of additional reagents required to separate or detoxify these intermediates makes processing lignin impractical. We report progress towards the use of such chemically depolymerized lignin streams by employing bacterial strains to produce polyhydroxyalkanoates (PHA). PHAs are a group of biodegradable microbial polyesters that have potential as a replacement for petroleum-based plastics. In this study we utilized two distinct lignin streams obtained after chemical depolymerization of lignin under alkaline and acidic pH in the presence of catalysts. We mixed the alkali-treated depolymerized stream with the acid-treated depolymerized stream to create a solution of neutral-pH chemically depolymerized lignin (CDL). We found moderate to substantial growth of both native and non-native PHA producers on the mixture of CDL as well as its aliphatic and aromatic components. PHA was detected by Sudan Black B staining in *C. necator* H16, *P. putida* KT2440, and *E. coli* LSBJ STQKAB grown on mixed CDL as the sole carbon source. For *C. necator* H16 and *E. coli* LSBJ STQKAB we found that PHA content was greater when grown on mixed CDL when compared to their preferred carbon source by GC-FID quantification. Our study provided progress towards a cost-competitive, sustainable, and industrially relevant use for lignin.
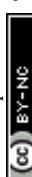
Sustainability spotlight

The cost-competitive and sustainable valorization of lignin, one of the most underutilized yet abundant sources of renewable carbon on Earth, represents a major opportunity in advancing circular biomanufacturing. This study addresses a key bottleneck in lignin bioconversion by integrating chemical depolymerization strategies with microbial biosynthesis to produce polyhydroxyalkanoates (PHAs), a family of biodegradable bioplastics. By combining base and oxidative catalytic depolymerized lignin streams, we broaden the chemical diversity and bioavailability of lignin-derived substrates. This process integration not only enhances microbial assimilation and product yields but also reduces the need for downstream pH adjustments, improving the overall environmental and economic viability of lignin valorization. Through systematic evaluation of native and engineered microbial strains, this work highlights a promising path toward upcycling lignin rich waste streams into sustainable, high value materials, supporting the transition to a defossilized and circular chemical industry aligning with UN SDG(s) 7, 9, 11, and 12.

[a]*Department of Bacteriology, University of Wisconsin–Madison, Madison, WI 53706, USA. E-mail: emajumder@wisc.edu*

[b]*Joint BioEnergy Institute, Emeryville, CA 94608, USA. E-mail: hchoudhary@lbl.gov; hchoudh@sandia.gov*

[c]*Department of Chemical Engineering, State University of New York College of Environmental Science and Forestry, Syracuse, NY 13210, USA*

[d]*Biological Systems and Engineering Division, Lawrence Berkeley National Laboratory, Berkeley, CA 94720, USA*

[e]*Department of Bioresource and Environmental Security, Sandia National Laboratories, Livermore, CA 94550, USA*

1. Introduction

The bioconversion of lignin, a structurally complex, and recalcitrant but largest renewable carbon source and the largest renewable source of aromatics on the planet, remains a major challenge in the development of cost-competitive biorefineries.[1–5] Unlike cellulose and hemicellulose, lignin resists microbial degradation due to its heterogeneous, cross-

linked structure and the predominance of non-hydrolysable C–C and C–O bonds.[6,7] Consequently, microbial valorization of lignin and lignin-derived substrates has typically suffered from limited carbon (bio)availability, low product titers, and poor conversion efficiencies.[3,8] While microbial engineering has made significant strides in enabling polymeric lignin or depolymerized lignin streams utilization, the scarcity of bioavailable intermediates remains a central bottleneck.[9,10]

To overcome this limitation, recent research has explored coupling chemical depolymerization with microbial conversion as a two-step strategy to access and valorize lignin carbon.[11–14] However, most studies have relied on a single chemical process to depolymerize lignin, resulting in a narrow distribution of bioavailable monomers or oligomers.[15] This limited chemical diversity restricts microbial uptake pathways and can reduce the overall carbon flux toward value-added products, such as polyhydroxyalkanoates (or PHAs, a biodegradable plastics).[10,16,17] As a result, the expected synergy between chemical depolymerization and microbial upgrading is frequently underrealized, with microbial titers remaining suboptimal.[18,19] PHAs, a biodegradable polyester, are a promising class of products that offer a renewable alternative to petrochemical plastics. Engineered microbial hosts have been developed to assimilate lignin-derived aromatics into PHA, yet success has been constrained by poor substrate compatibility, inhibitory byproducts, and a lack of tunable feedstock composition.[20–22]

The biological processing of lignin provides its own multitude of opportunities and challenges to utilize lignin. Many microbes have the capacity to use aromatic compounds for both carbon and energy sources and contain well described pathways for aromatic ring degradation such as dioxygenase mediated ring open reactions found in the homogentisate pathway of *Psuedomonas putida*.[8,23] Lignin aromatic monomers, *e.g.* benzoate, in high concentrations are toxic to most microbes and many fermentation strategies include glucose as a carbon source for growth which can induce catabolic repression of pathways involving aromatic compounds.[8] However, some microbes can funnel the metabolic products of aromatic degradation towards industrially relevant compounds such as triglycerides and PHAs. Previous literature has shown that microbial strains, especially strains of *P. putida* and *C. necator*, can produce PHAs from a range of substrates such as plastic waste, lignocellulosic material, spent coffee grounds, and even slaughterhouse waste.[24–26] Conversion of lignocellulosic material to PHAs is well described for the cellulosic component, often yielding the most PHA whereas conversion of lignin is less well described and often results in lower yields.[27] Additionally, many studies investigating lignin conversion to PHA have looked only at kraft lignin or individual lignin derivatives as the substrate for microbial production of PHAs rather than an industrially relevant mixture of lignin depolymerization products.[27]

Motivated by this, we aimed to demonstrate the production of a valuable bioproduct from lignin waste by implementing process-advantaged steps that integrate chemical and biological processing. We strategized to combine two different chemically depolymerized lignin (CDL) streams, one from a base catalyzed

depolymerization (BCD) and another from an oxidative catalytic depolymerization (OCD) processed at different pH values, to enhance the substrate diversity and reduce the downstream pH adjustment costs. By integrating chemically complementary depolymerized lignin streams, that is more readily consumed (aliphatics) and more complex to breakdown (aromatics), we expanded the pool of bioavailable molecules and promoted metabolic synergy within a microbial host capable of PHA biosynthesis. We also compared the performance of native PHA producers and engineered microbial chassis across different lignin streams. As discussed later, this combined chemistry approach significantly boosts microbial uptake and PHA production, offering a promising framework for lignin valorization through integrated chemical and biological processing. The PHA-producing strains used in this study were chosen for known aromatic metabolism, tolerance and metabolism of diverse carbon sources and PHA production. Native producers are *Pseudomonas putida* KT2440, *Cupriavidus necator* H16, and *Thermus thermophilus* HB27, and one engineered *Escherichia coli* LSBJ pBBR STQKAB. Growth was seen from all strains on the mixed CDL as well as individual aliphatic and aromatic lignin depolymerization streams. PHAs were produced on the mixed CDL medium by three strains and native producers biosynthesized higher value medium chain length PHAs than on sugar as the carbon source. When quantified, *E. coli* LSBJ pBBR STQKAB produced the most PHAs from the mixed CDL with ∼30% of the cell dry weight being PHB.

2. Methods

2.1 Lignin processing and characterization

2.1.1. Generation of lignin-rich solids. Cholinium lysinate ([Ch][Lys])-based pretreatment of poplar biomass and subsequent saccharification was performed in a one-pot configuration in a 1 L Parr 4520 series bench top reactor (Parr Instrument Company, Moline, IL) as described elsewhere.[28] Briefly, poplar, [Ch][Lys], and water were mixed in a 3 : 2 : 15 ratio (w/w) in the Parr vessel to achieve 15 wt% solid loading. This slurry mixture was pretreated for 3 h at 160 °C with stirring at 80 rpm powered by process (Parr Instrument Company, model: 4871, Moline, IL) and power (Parr Instrument Company, model: 4875, Moline, IL) controllers using three-arm, self-centering anchor with PTFE wiper blades. After 3 h, the pretreated slurry was cooled down to room temperature. The pH of the cold, pretreated mixture was adjusted to 5 with 72% sulfuric acid. Enzymatic saccharification was carried out at 50 °C for 72 h at 80 rpm using enzyme mixtures Cellic CTec3 and HTec3 (9 : 1 v/v) at a loading of 20 mg protein per g biomass. After 72 h, polysaccharides in the poplar biomass were hydrolyzed into monomeric sugars. The slurry was centrifuged for solid–liquid separation followed by water washing until the pH of the colorless washing was neutral. The washed material was freeze dried to obtain lignin-rich solids.

2.1.2. Catalytic oxidation of lignin-rich solids into aliphatic acids (OCD stream). The oxidative depolymerization of lignin was achieved as described previously.[29] Lignin-rich solids, polyoxotungstate catalyst, hydrogen peroxide, and water were mixed in a ratio of 3 : 1 : 6 : 40 (w/w), pressurized with 100 psi N_2

and heated at 140 °C for 1 h. The poplar-based lignin-rich solid was used to generate a OCD stream in a 1 L Parr reactor. After 1 h, unreacted solids were separated from the aqueous stream containing depolymerized bioavailable products by centrifugation. The aqueous stream containing depolymerized products was filtered through 0.45 μm SFCA sterile filter units. The filtered lignolysate (OCD stream) was used for bioproduction studies. The aqueous stream containing depolymerized products was analyzed using an Agilent HPLC 1260 infinity system (Santa Clara, California, United States) equipped with a Bio-Rad Aminex HPX-87H column and a refractive index detector at 35 °C. An aqueous solution of H_2SO_4 (4 mM) was used as the eluent (0.6 mL min^{-1}, column temperature 60 °C).

2.1.3. Base-catalyzed depolymerization of lignin-rich solids into aromatic acids (BCD stream).

The poplar-based lignin-rich solid was used to generate a BCD stream in a 1 L Parr reactor.[14,30] Lignin solids (15 wt%) and 5 wt% sodium hydroxide (aqueous solution) were added to the Parr vessel and the temperature was ramped up to 120 °C in 30 min. The temperature was held at 120 °C for 30 min with vigorous stirring at 80% output of the rotor. After 30 min, the reactor was cooled down and unreacted solids were separated from the aqueous stream containing depolymerized bioavailable products by centrifugation. The aqueous stream containing depolymerized products was filtered through 0.45 μm SFCA sterile filter units. The filtered lignolysate (BCD stream) was used for bioproduction studies. The acid content in the BCD stream was analyzed, as described previously,[14] on a 1260 Infinity II (Agilent Technologies) equipped with an Eclipse Plus Phenyl-Hexyl column (250 mm length, 2.6 mm diameter, 5 μm particle, Agilent Technologies, 95990-912), and a UV detector. Two mobile phases were used, 10 mM ammonium acetate with 0.07% formic acid in water (Solvent A) and 10 mM ammonium acetate with 0.07% formic acid in 90% acetonitrile (Solvent B). The profile mixture was as follows: 30% Solvent B, 0.5 mL min^{-1} for 12 min, 80% Solvent B, 0.5 mL min^{-1} for 0.1 min, 100% Solvent B, 0.5 mL min^{-1} for 0.5 min, 100% Solvent B, 1.0 mL min^{-1} for 0.2 min, and 30% Solvent B, 1.0 mL min^{-1} for 2.8 min. The column temperature was kept at 50 °C. p-Coumaric acid concentrations were compared against analytical standards at a 254 nm spectral profile. 4HBA concentrations were compared against analytical standards at a 280 nm spectral profile and PCA concentrations were compared against analytical standards at a 310 nm spectral profile.

2.2 Growth media, bacterial strains and cultivation conditions

All reagents were purchased from Sigma-Aldrich unless otherwise designated. M9 media was created using a 10X Salt stock containing 128.48 g L^{-1} Na_2HPO_4, 30 g L^{-1} KH_2PO_4, 10 g L^{-1} NH_4Cl (purchased from Dot Scientific), 5 g L^{-1} NaCl pH 7.0 was diluted to 1X with autoclaved MilliQ water. The 1X salt stock was mixed with 1 M $MgSO_4$ to a final concentration of 1 mM $MgSO_4$ and a trace element solution containing $FeCl_3$, $CaCl_2$, $CoCl_2$, $CuSO_4$, $NiCl_3$, $CrCl_3$. Thermus minimal media (TMM) contained 0.50 g L^{-1} K_2HPO_4, 0.30 g L^{-1} KH_2PO_4, 0.50 g NH_4Cl, 0.50 g L^{-1}

NaCl, 0.20 g L^{-1} $MgCl_2 \cdot 6H_2O$ (purchased from Fischer Scientific), 0.04 g L^{-1} $CaSO_4 \cdot 2H_2O$ (purchased from Ward's Science+), 40 mM Tris, Wolfe's minerals (purchased from ATCC), and Wolfe's vitamins (purchased from ATCC) with a pH of 7.2. Minimal media containing 10 mM glucose was used as a positive control, and minimal media containing 10 mM fructose was used as a positive control for C. necator H16.

A solution of mixed CDL was created by neutralizing a waste stream of OCD lignin with a waste stream of BCD lignin to a pH of 7.0 or 7.2 (T. thermophilus HB27) in MilliQ water. The amount of each stream mixed was calculated based on trying to match the total amount of carbon in the medium to the glucose or fructose minimal media control condition. The final pH was adjusted as necessary using 6 M NaOH or 6 M HCl and was determined using a FischerBrand Accumet Liquid-Filled bench top pH probe. The CDL was diluted with M9 or Thermus minimal media (TMM) and vacuum filtered to achieve the desired concentrations seen in Table 1.

A variety of bacterial strains from the Majumder Lab collection, unless source noted, were used in this study to produce PHAs from a mixture of CDL. Natural producers of PHAs were studied using the mesophiles Cupriavidus necator H16 and Pseudomonas putida KT2440 and the thermophile Thermus thermophilus HB27 (DSM 7039) (purchased from ATCC as freeze-dried cells). Engineered PHA producers were studied using E. coli LSBJ bearing the PHB biosynthesis plasmid pBBR STQKAB, which contains the phaA, phaB, and phaC1 genes for PHB production as well as kanR as a selection marker, while E. coli LSBJ without the PHB biosynthesis pathway was used as a PHB negative control.[31]

To bring cultures up from freezer stocks, C. necator H16, P. putida KT2440, and E. coli LSBJ were grown overnight in rich media cultures using LB Broth Miller (Luria–Bertani) from Fisher Scientific. T. thermophilus HB27 was grown overnight using Thermus Enhanced Media (TEM) using ATCC medium 1598 recipe. All E. coli LSBJ pBBR STQKAB cultures contained 50 mg L^{-1} Kanamycin. For overnight, growth curve and production experiments, T. thermophilus HB27 was grown at 70 °C and shaking at 200 rpm whereas C. necator H16, P. putida KT2440, and E. coli LSBJ were grown at 30 °C and shaking at 200 rpm.

Growth curves were obtained using triplicate 5 mL cultures in capped borosilicate tubes. OD600 was measured at 2-hour time points with a ThermoScientific Genesys 50 UV/vis spectrophotometer. Initial growth rates were calculated using the linear portion of the log growth phase from a semi-log plot of the growth curve. Measurement of carbon sources remaining after cultivation was carried out by HPLC as described in Sections 2.1.2 and 2.1.3.

2.3 Staining of PHA granules

Sudan Black B staining was conducted following the protocol developed in Burdon, 1946 with modifications.[32] Cells were taken from 100 mL shake flask cultures after 48 h then dried and heat fixed onto glass slides. Cells were stained with a 3% Sudan Black B (Sigma Aldrich) solution (0.3 g in 100 mL of 70%

Table 1 Composition of and total carbon present in the prepared CDL minimal media and glucose minimal media

Compound	Aromatic CDL (mM)	Aliphatic CDL (mM)	Mixed CDL (mM)	Glucose or fructose (mM)
Succinate	0.004	0.030	0.032	—
Malate	0.022	0.019	0.028	—
Malonate	0.006	2.676	2.741	—
Oxalate	0.014	4.850	4.969	—
Acetate	—	9.422	9.643	—
Formate	—	19.653	20.114	—
4-Hydroxybenzaldehyde	0.035	0.000	0.014	—
Protocatechuic acid	0.000	0.006	0.006	—
4-Hydroxybenzoic acid	0.918	0.004	0.371	—
Protocatechuic acid	0.000	0.006	0.006	—
4-Hydroxybenzoic acid	0.918	0.004	0.371	—
Syringic acid	0.102	0.001	0.042	—
Vanillic acid	0.103	0.026	0.068	—
p-Coumaric acid	0.008	0.000	0.003	—
Sinapic acid	0.010	0.000	0.004	—
Ferulic acid	0.015	0.000	0.006	—
Vanillin	0.170	0.000	0.068	—
Syringaldehyde	0.163	0.000	0.065	—
Glucose or fructose	—	—	—	10
Total C in 500 mL (g)	0.071	0.341	0.377	0.360

EtOH) by flooding the slide for 10 minutes. Slides were rinsed with DI water and destained ethanol. Safranin was used to counterstain the cells for 30 seconds and slides were rinsed with DI water. Slides were viewed under a 100X oil-immersion lens on a FisherBrand Research Grade Upright Microscope. The presence of PHA granules that accumulate in the cytoplasm of cells are visualized as black granules within the cells or as black-blue stained cells.[33]

2.4 PHA production, extraction, and quantification

Cultures of *Cupriavidus necator* H16, *Pseudomonas putida* KT2440, *Escherichia coli* LSBJ pBBR STQKAB, and *E. coli* LSBJ were grown in 100 mL M9 minimal media supplemented with CDL, glucose, or fructose as the sole carbon source. Cultures were grown for 48 h at 30 °C and shaking at 200 rpm. Cells were pelleted at 5031 rcf in a centrifuge for 10 minutes and then frozen for 24 h at −80 °C. Frozen cells were lyophilized. After lyophilization, 10–30 mg of dried cells were weighed out and mixed with 2 mL Chloroform and 2 mL 15% (v/v) sulfuric acid in methanol in a glass screw cap pressure vial. The mixture was then heated to 100 °C for 150 minutes. After cooling 1 mL of MilliQ water and 500 μl of 0.25% (v/v) Methyl Benzoate in chloroform was mixed by vertexing. Aqueous and organic layers were separated by centrifugation at 44 rcf for 5 minutes. The organic layer was passed through a 0.2 μm poly-tetrafluoroethylene filter into 2 mL GC vials. Samples were analyzed using a Shimadzu GC 2010 Gas Chromatograph with an AOC-20i autoinjector and a flame ionization detector with a Restek RTX-5 column. Samples were run in split mode (40 : 1) with an injection volume of 1 μL and an injection temperature of 280 °C, a detector temperature of 310 °C, and a heating profile for the oven as follows: 100 °C for 7 min, ramp 8 °C min⁻¹ to 280 °C, hold for 2 min, ramp 20 °C min⁻¹ to 310 °C, hold for 2 min. Chromatographic data were analyzed using the locally installed instrument software, Chromeleon. These polymers are often classified as short-chain-length (SCL) PHAs which consist of C_3–C_5 monomers and medium-chain-length (MCL) PHAs which consist of C_6–C_{14} monomers. The most common SCL-PHAs are poly(3-hydroxybutyrate) (PHB), C_4 and poly(3-hydroxyvalerate) (PHV), C_5, and the most common MCL-PHAs are poly(3-hydroxyoctanoate) (PHO), C_8, and poly(3-hydroxynonanoate) (PHN), C_9 (see SI). Additionally, there can be co-polymers which consist of two different monomer types within the same polymer, the most common of which is poly(3-hydroxybutyrate-*co*-3-hydroxyvalerate) (PHBV).[16] PHAs were characterized by comparison to a standard curve using the methyl esters of the common PHA monomers that would be the result of acidic methanolysis: methyl-3-hydroxybutanoate, methyl-3-hydroxyvalerate, methyl-3-hydroxyheptanoate, methyl-3-hydroxyoctanoate, and methyl-3-hydroxydecanoate corresponding to PHB, PHV, PHHp, PHO, and PHD respectively.

3. Results

3.1 Microbial growth on chemically depolymerized lignin (CDL) media

After chemically depolymerizing the lignin, the BCD process resulted in an aromatic rich stream with a pH of 12. The most abundant compounds within the aromatic stream are 4-hydroxybenzoic acid, vanillin, syringaldehyde, vanillic acid, and syringic acid (Table 1). The OCD process resulted in an aliphatic rich stream with a pH of 2. The most abundant compounds within the aliphatic stream are formate, acetate, oxalate, malonate, and succinate (Table 1). Given that BCD was basic and OCD was acidic, a mixed media condition (Table 1) was created to self-neutralize and reduce the amount of acid or base added during the microbial conversion step. It is worth mentioning that the amount and type of aromatic acids (from BCD) and aliphatic acids (from OCD) depend on the lignin source

employed. For instance, as reported in our previous study, the hardwood lignin generated considerably higher amounts of formic acid than the softwood lignin after the OCD process.[29] Similarly, higher concentrations of coumarate were observed in grassy lignin compared to hardwood poplar lignin after BCD treatment.[14,30] The variance in the products of the depolymerized stream as a function of lignin source has a cascading impact on microbial growth profiles as well as on the titers of the bioproduct.

To test the growth of the native (*P. putida* KT2440, *C. necator* H16, *T. thermophilus* HB27) and engineered (*E. coli* LSBJ STQKAB) PHA-producing microbial strains, aromatic, aliphatic, and mixed streams of CDL were used as the sole carbon source in minimal media. Microbial growth on the CDL media was compared to growth negative control without a carbon source and a glucose or fructose positive control (Fig. 1). Very little growth was observed for any strain on the no carbon source media condition, as expected. For almost all conditions with growth, little to no lag phase was observed. Growth did vary between the microbial strains on CDL and the type of CDL used as the sole carbon source. Initial growth rates on all CDL-based media were either somewhat reduced or similar when compared to growth rates on glucose or fructose as the sole carbon source for the three mesophilic bacteria tested (Table 2).

Likewise, among the CDL-containing conditions, the three mesophiles tended to show growth rate increases in the presence of the aliphatic stream from the OCD process, whereas the thermophile *T. thermophilus* HB27 grew the slowest and in the presence of the aliphatic stream had a very long lag phase suggesting the stream is toxic to this bacterium. *P. putida* KT2440 had the slowest growth rates of the three mesophiles for all media types. *E. coli* LSBJ STQKAB and *C. necator* similar growth rates that were highest for the CDL-containing conditions in the mixed CDL media at 0.50 and 0.47 h^{-1}, respectively (Table 2).

In addition to initial growth rates, we also examined growth performance by comparing differences in maximum Optical Density (OD). Highest maximum ODs were observed for the preferred carbon source media condition in all strains and were around 1. *P. putida* KT2440, *E. coli* LSBJ STQKAB, and *C. necator* H16 showed substantial growth with mixed CDL as the sole carbon source (Fig. 1) reaching maximum optical densities at 600 nm (OD_{600}) of 0.58, 0.57, and 0.74, respectively (Fig. 1, Table 3). Whereas *T. thermophilus* HB27 showed greatly reduced growth with mixed CDL as the sole carbon source, reaching a final OD_{600} of only 0.21. Growth for *P. putida* KT2440, *E. coli* LSBJ STQKAB, and *C. necator* H16 on each of the individual streams of aromatic CDL and aliphatic CDL had around half the biomass when
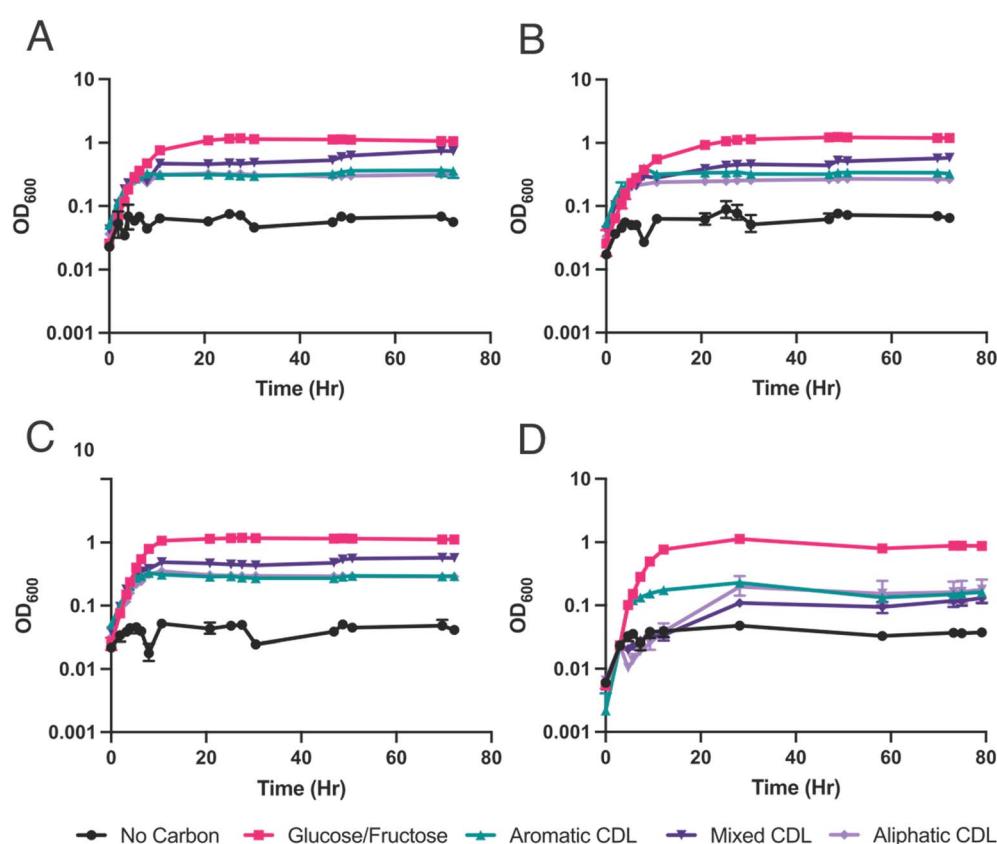

Fig. 1 Growth curve of native and engineered PHA producing strains on CDL as the sole carbon source in minimal media. Black line represents inoculation in minimal media with no carbon source. Pink line represents growth on minimal media with a preferred carbon source, glucose or fructose (*C. necator* H16). Teal represents growth on minimal media with the aromatic CDL as the sole carbon source. Dark purple represents growth on minimal media with the mixed CDL as the sole carbon source. Light purple represents growth on minimal media with the aliphatic CDL as the sole carbon source. (A) *C. necator* H16, (B) *P. putida* KT2440, (C) *E. coli* LSBJ STQKAB, (D) *T. thermophilus* HB27. N = 3.

Table 2 Growth rates of native and engineered PHA producers on CDL media and preferred carbon source media. Average ± SD, N = 3; bld: below limit of detection. Preferred carbon source: glucose or fructose (*C. necator* H16)

Microbial strain	Growth rate on preferred carbon source (h^{-1})	Growth rate on aromatic CDL (h^{-1})	Growth rate on aliphatic CDL (h^{-1})	Growth rate on mixed CDL (h^{-1})	Final pH of mixed CDL media
C. necator H16	0.45 ± 0.02	0.38 ± 0.04	0.46 ± 0.02	0.47 ± 0.04	7.77 ± 0.05
P. putida KT2440	0.42 ± 0.05	0.33 ± 0.005	0.40 ± 0.01	0.33 ± 0.004	7.77 ± 0.05
E. coli LSBJ STQKAB	0.64 ± 0.04	0.41 ± 0.03	0.47 ± 0.09	0.50 ± 0.01	7.38 ± 0.02
T. thermophilus HB27	0.39 ± 0.01	0.092 ± 0.006	bld	bld	6.92 ± 0.08

Table 3 Final OD of native and engineered PHA producers on CDL media and preferred carbon source media. Average ± SD, N = 3; preferred carbon source: glucose or fructose (*C. necator* H16)

Microbial strain	Final OD			
	Preferred carbon source	Mixed CDL	Aromatic CDL	Aliphatic CDL
C. necator H16	1.06 ± 0.04	0.74 ± 0.02	0.36 ± 0.07	0.32 ± 0.03
P. putida KT2440	1.20 ± 0.02	0.58 ± 0.02	0.33 ± 0.01	0.27 ± 0.01
E. coli LSBJ STQKAB	1.15 ± 0.08	0.57 ± 0.01	0.29 ± 0.02	0.029 ± 0.004
T. thermophilus HB27	0.88 ± 0.05	0.13 ± 0.02	0.16 ± 0.01	0.18 ± 0.07

compared to the mixed CDL media. *T. thermophilus* HB27 showed similar growth, if not slightly more, on the aromatic CDL when compared to the mixed CDL with a maximum OD$_{600}$ of 0.23 and reduced growth on the aliphatic CDL with a maximum OD$_{600}$ of 0.10 but were still less than the mesophiles. However, if we consider that the aliphatic CDL medium has only about 20% of the carbon available as the other two CDL-containing media tested and that some strains reached similar maximum ODs, it suggests that the strains can more efficiently use the carbon sources available in the aliphatic stream.

Given this observation of carbon utilization, we tested the spent medium for the amount of remaining carbon at different time points. Of the various carbon sources present, in the prepared medium, only formate and acetate were above the HPLC detection limit in most media tested (6 of 9) (Table S1). Formate but not acetate was only detected in two of the conditions after the first inoculated time point suggesting that in most cases the bacteria are readily utilizing these two carbon sources. For *P. putida* KT2440 on the aliphatic CDL stream, the concentration of formate fluctuated and ended above the starting concentration suggesting that both were being produced and consumed by the bacterium over the course of the growth curve. The other condition with remaining formate was again the aliphatic CDL stream but with *E. coli* LSBJ STQKAB. In this case, concentration of formate decreased over time but only about 16% was consumed. The final pH of the cultures was also measured for the mixed CDL condition. The pH went up slightly for the three mesophiles and was still approximately 7 for the thermophile (Table 2). An increase in pH can be associated with PHA production or the removal of acidic molecules from the medium.

3.2 PHA detection

Based on the performance in the growth trials, the mixed CDL as the sole carbon source condition was selected for PHA

production testing. After 48 hours of growth, cells were harvested and PHA granules were detected by Sudan Black B staining (Fig. 2). Black-stained PHA granules are observed in *C. necator* H16, *P. putida* KT2440, and *E. coli* LSBJ STQKAB cells grown in mixed CDL media (Fig. 2A–C) and on their respective preferred sugar medium (Fig. 2E–G). As expected, black granules were not present in PHB negative strains of *E. coli* nor in the uninoculated media controls (Fig. 2I–L). However, unexpectedly, PHA granules cells nor black-blue stained cells were not detected for the native PHA producer *T. thermophilus* HB27 when grown in the mixed CDL as the sole carbon source (Fig. 2D). The *T. thermophilus* HB27 cells in the glucose medium appeared to be more purple but were inconclusive (Fig. 2H).

3.3 PHA quantification and characterization

For the conditions where PHA granules were detected by staining, GC-FID was used to quantify the amount of PHAs and identify the PHA monomers produced by the microbial cultures after extraction. Samples were run in biological duplicate for the mixed CDL and preferred carbon source conditions, fructose for *C. necator* H16 and glucose for all other strains (Table 4). For native PHA producers, the types of PHAs produced tended to include longer chain PHAs such as PHD and PHV when grown on mixed CDL compared to PHB on a sugar carbon source. Interestingly, the two replicates for *P. putida* KT2440 grown on 10 mM glucose were found to have generated two different PHAs with one making PHV and the other PHD. In terms of yield, *C. necator* H16 produced twice as the amount of PHAs and biomass on mixed CDL than fructose while *P. putida* KT2440 had the opposite trend of yielding more PHAs and biomass on glucose than mixed CDL (Table 4). Biological replicates of *T. thermophilus* HB27 grown on 10 mM glucose produced PHB at an average concentration of 41.2 ± 30.8 mg L^{-1} comprising 7.0 ± 5.7% of CDW, which was less than the mesophile native PHA producers tested. *T. thermophilus* HB27 was not tested on mixed
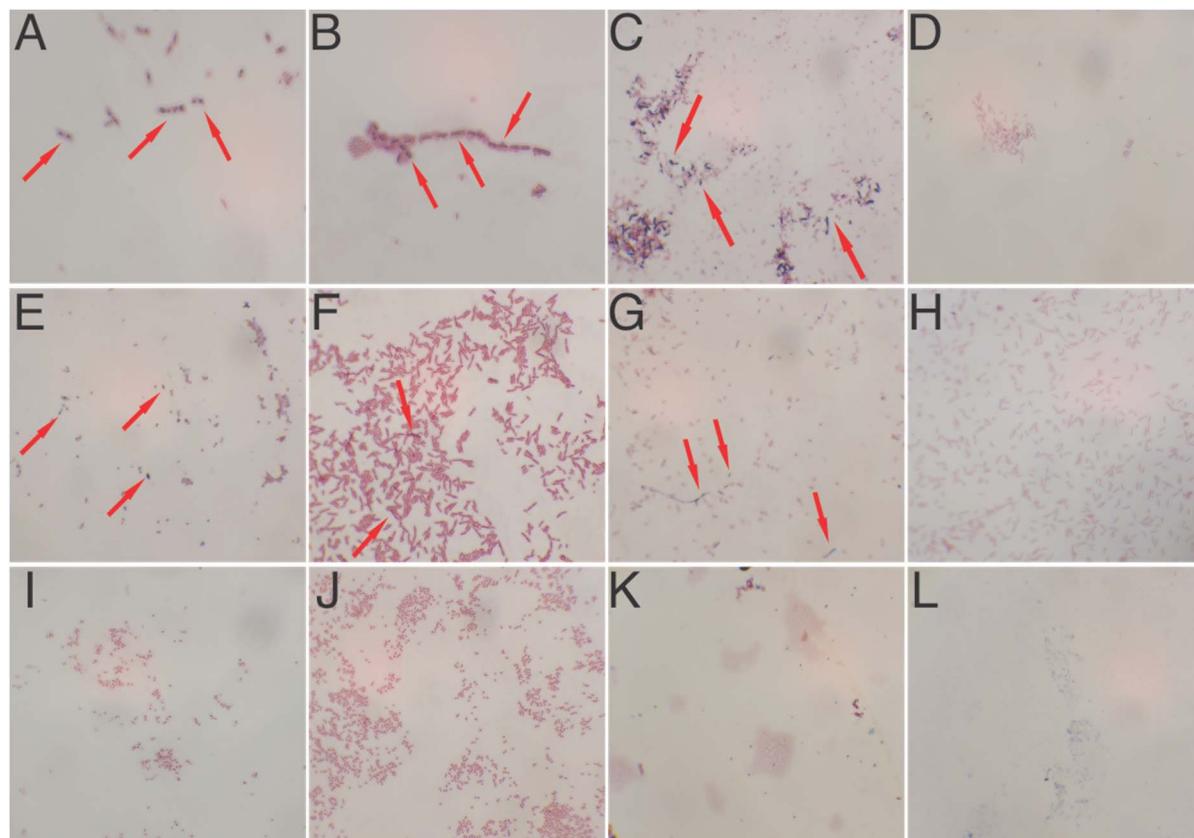
Fig. 2 Sudan Black B stain of strains at stationary phase on mixed CDL in minimal media. Arrows point out PHA granules visualized by the Sudan Black B dye. (A) *C. necator* H16 on mixed CDL, (B) *P. putida* KT2440 on mixed CDL, (C) *E. coli* LSBJ STQKAB on mixed CDL, (D) *T. thermophilus* HB27 on mixed CDL. (E) *C. necator* H16 on 10 mM fructose, (F) *P. putida* KT2440 on 10 mM glucose, (G) *E. coli* LSBJ STQKAB on 10 mM glucose, (H) *T. thermophilus* HB27 on 10 mM glucose. Negative controls: (I) *E. coli* LSBJ PHB- (no plasmid) on mixed CDL, (J) *E. coli* LSBJ PHB- on 10 mM glucose, (K) mixed CDL media, uninoculated, (L) M9 minimal media, uninoculated.

CDL due to lower growth and absence of a positive Sudan black stain. For the engineered strain, *E. coli* LSBJ STQKAB grown on mixed CDL produced substantially more PHB, 337.0 ± 51.1 mg L^{-1} comprising 30.4 ± 0.1% of CDW, than when grown on 10 mM glucose yielding only 85.7 ± 3.5 mg L^{-1} and 16.3 ± 1.2% of CDW. *E. coli* LSBJ STQKAB grown on mixed CDL was also the highest tested condition overall in this study for biomass and PHA production metrics.

4. Discussion

All strains tested show some degree of growth on each of the chemically depolymerized lignin. In most cases, the most robust growth was seen in the mixed CDL media that contained both the aliphatic and aromatic waste-streams. *C. necator* H16 showed the most growth out of all the strains on the mixed CDL media, which is likely due to the presence of many aromatic and aliphatic degradation pathways in this bacterium. *P. putida* KT2440 similarly, has many aromatic degradation pathways which can explain the robust growth on the aromatic waste stream. However, surprisingly, *P. putida* KT2440 had the slowest growth rates out of all the mesophiles on every media condition; glucose included. In a related finding, previous work done on *P.*

putida KT2440 strains isolated from the environment had lower growth rates on individual lignin components ranging from 0.22 ± 0.007 h^{-1} to 0.27 ± 0.004 on benzoate (Ravi *et al.*, 2017).[34] *E. coli* LSBJ STQKAB grew similarly on both the aliphatic and aromatic waste streams with slightly higher and faster growth on the aliphatic media. *T. thermophilus* HB27 showed the lowest and the slowest growth of all strains on each of the chemically depolymerized lignin carbon sources. For these heterogenous CDL streams, there are many carbon sources present. Some compounds in the mixture may promote faster growth due to direct incorporation in pathways associated with biomass production such as central carbon metabolism. Small organic acids such as acetate or malate can contribute directly to the TCA cycle and malonate can contribute to fatty acid anabolism, whereas the aromatics like 4-hydroxybenzoic acid or vanillic acid must go through aromatic ring opening and further pre-processing before being able to contribute to central metabolic pathways.[3,6] Thus, it was expected to see a reduced growth rate in the aromatic only stream when compared to the aliphatic stream or the mixed CDL, which also contained these small organic acids.

There are stark differences between the quantity and characteristics of the PHA produced in the engineered *E. coli* LSBJ

Table 4 Quantification and characterization of PHA. PHA quantification by GC–FID, cell dry weight (CDW), % content of PHA in CDW, and type of PHA polymer for native and engineered PHA producers on their preferred carbon source and mixed CDL. $N = 2^a$

Strain	Condition	CDW (mg L^{-1})	PHA (%CDW)	PHA yield (mg L^{-1})	PHAs detected[b,c]
C. necator H16	10 mM fructose	755 ± 35.36	10.95 ± 0.35	82.35 ± 1.20	PHB
C. necator H16	Mixed CDL	855 ± 601.04	17.1 ± 1.13	149.2 ± 112.15	PHB (53.6%); PHV (46.4%)
P. putida KT2440[d]	10 mM glucose	610 ± 98.99	4.95 ± 5.3	27.6 ± 27.58	PHV; PHD
P. putida KT2440	Mixed CDL	525 ± 205.06	0.65 ± 0.64	2.85 ± 2.05	PHD
E. coli LSBJ STQKAB	10 mM glucose	530 ± 84.85	16.3 ± 1.7	85.65 ± 4.88	PHB
E. coli LSBJ STQKAB	Mixed CDL	1025 ± 120.2	30.45 ± 0.07	336.95 ± 72.2	PHB
T. thermophilus HB27	10 mM glucose	680 ± 155.56	6.95 ± 7.99	41.15 ± 43.49	PHB
T. thermophilus HB27	Mixed CDL	Not detected	—	—	—

[a] A significant large standard deviation was observed when replicates produced different PHAs or when cells were very stressed and produced low yields. PHB is poly(3-hydroxybutanoate). PHV is poly(3-hydroxyvalerate). PHD is poly(3-hydroxydecanoate). [b] Percent shown if more than one monomer was detected. If monomer composition varied in each replicate, monomer content separated by semicolon. [c] PHA composition is shown on the basis of monomers detected using GC-FID. [d] Two different monomers were detected in two different replicates with glucose as the feed.

STQKAB and the native producers *C. necator* H16 and *P. putida* KT2440. *E. coli* LSBJ STQKAB showed the highest yield of PHB produced on the mixed CDL media and largest percentage of PHB in the CDW. The higher yields and higher percentage of CDW are attributed to PHB to the engineered strain not containing a pathway for degrading the PHB within the cell. The native PHA producers can both build and depolymerize the PHAs made within the cell, which can lower the yield of PHA. Likewise, only PHB was observed for *E. coli* LSBJ STQKAB because the PHA-producing genes on the inserted plasmid only function for PHB. The characteristics of the PHAs produced in the native strains also differed. *C. necator* H16 mainly produces SCL-PHAs such as PHB and PHV, whereas *P. putida* KT2440 produces mainly MCL-PHAs such as PHO and PHD.[35–37] The results of this study corroborate the differences in PHA production between these two organisms with *C. necator* H16 mainly producing PHB and PHV, while *P. putida* KT2440 was shown to produce PHD. Longer chain PHAs can be used to produce bioplastics that are more flexible whereas SCL-PHAs are more brittle and have applications similar to polypropylene. Likewise, PHB can already be made commercially but it is desirable to produce it from a waste stream to reduce costs. Since MCL-PHAs were produced from lignin waste streams here in native producers and the engineered strain had good yields of PHB, this could be a more valuable bioconversion route.

When compared to other studies, the PHA yields of the native producers, *P. putida* KT2440 and *C. necator* H16, have lower percent of CDW values than typically reported. A brief report of *P. putida* KT2440's ability to produce PHA from lignin-containing carbon sources, corn stover, and lignin derivatives such as *p*-coumaric acid or ferulic acid, showed that PHA yields ranged from 8.8 to 41% of CDW.[38] A review of *C. necator* as a platform for PHA production showed that wildtype *C. necator* H16, on a variety of substrates, had PHA yields of up to 82% of CDW.[36] PHA production can be optimized through methods such as batch-feeding,[39] use of bioreactors, nitrogen limitation, control of redox state,[27] and mixotrophic growth of *C. necator*.[40]

Any of these methods would be likely to improve yields in the conditions tested here. Interestingly more of the CDW was PHA in the mixed CDL condition for *E. coli* LSBJ STQKAB and *C. necator* H16. Furthermore, *E. coli* demonstrated superior selectivity toward Mixed CDL stream over glucose, achieving ~70% carbon recovery, while *C. necator* showed a similar carbon recovery profile (52–57%) for both Mixed CDL and its preferred carbon source, *i.e.*, glucose (see Table S2). In contrast, *P. Putida* and *T. thermophilus* preferred glucose as a substrate exhibiting limited to no carbon recovery. The increase in PHA content in this case could be due to upregulation of PHA biosynthesis during stress events caused by either the lack of preferred carbon sources or the presence of toxic aromatics or acidic small molecules. This project showed that PHAs can be produced from a self-neutralizing mixture of lignin derivatives generated from different sustainable chemical processes. Collectively, these findings suggest that an integrated biorefinery utilizing both carbohydrate and lignin fractions could provide distinct economic and environmental advantages over conventional pathways—a hypothesis we intend to validate through future techno-economic analysis and detailed life cycle assessment analyses.

5. Conclusion

Taken together, the results of this study show that chemically depolymerized lignin (CDL) can be used as substrate for microbial growth and bioconversion, thus giving a route for bioproduction of industrially relevant substances from a cost effective, waste feedstock. This study demonstrated the production of the bioplastic polymer class polyhydroxyalkanoates (PHA), by both native and engineered microbes. We found that both the native and engineered microbes were able to grow and produce multiple types of PHAs on the mixed CDL. Native PHA-producing bacteria showed advantages in producing the more valuable MCL-PHAs while the engineered train demonstrated advantage in PHA yield. The aliphatic CDL stream promoted faster growth but both aromatic and CDL streams supported similar maximum ODs. The

mixture of the two streams gave the best growth and production results. In the future, stream mixing and growth conditions can be optimized for higher PHA yields and better selection of the type of PHA produced.

Conflicts of interest

HC and ELWM are named inventors on at least one related patent application. BAS has a financial interest in Illium Technologies, Caribou Biofuels, and Erg Bio. None of the other authors have any outside financial interests.

Note added after first publication

This article replaces the version published on 2nd October 2025, which incorrectly included a structure image in the final column of Table 4.

Data availability

All data are published within the manuscript or SI. The SI contains a table characterizing the remaining carbon sources in the spent media, calculation of carbon balance, and images of polymer structures.

Supplementary information is available. See DOI: https://doi.org/10.1039/d5su00563a.

Acknowledgements

References

1 R. Patel, P. Dhar, A. Babaei-Ghazvini, M. Nikkhah Dafchahi and B. Acharya, *Bioresour. Technol. Rep.*, 2023, **22**, 101463.

2 H. Luo and M. M. Abu-Omar, in *Encyclopedia of Sustainable Technologies*, Elsevier, 2017, pp. 573–585.

3 S. Shrestha, S. Goswami, D. Banerjee, V. Garcia, E. Zhou, C. N. Olmsted, E. L.-W. Majumder, D. Kumar, D. Awasthi, A. Mukhopadhyay, S. W. Singer, J. M. Gladden, B. A. Simmons and H. Choudhary, *ChemSusChem*, 2024, **17**, e202301460.

4 A. J. Ragauskas, G. T. Beckham, M. J. Biddy, R. Chandra, F. Chen, M. F. Davis, B. H. Davison, R. A. Dixon, P. Gilna, M. Keller, P. Langan, A. K. Naskar, J. N. Saddler, T. J. Tschaplinski, G. A. Tuskan and C. E. Wyman, *Science*, 2014, **344**, 1246843.

5 V. Jassal, C. Dou, N. Sun, S. Singh, B. A. Simmons and H. Choudhary, *Front. Chem. Eng.*, 2022, **4**, 1059305.

6 J. Ralph, C. Lapierre and W. Boerjan, *Curr. Opin. Biotechnol.*, 2019, **56**, 240–249.

7 M. M. Abu-Omar, K. Barta, G. T. Beckham, J. S. Luterbacher, J. Ralph, R. Rinaldi, Y. Román-Leshkov, J. S. M. Samec, B. F. Sels and F. Wang, *Energy Environ. Sci.*, 2021, **14**, 262–292.

8 G. T. Beckham, C. W. Johnson, E. M. Karp, D. Salvachúa and D. R. Vardon, *Curr. Opin. Biotechnol.*, 2016, **42**, 40–53.

9 M. E. Wolf and L. D. Eltis, *Trends Biochem. Sci.*, 2025, **50**, 322–331.

10 Z.-H. Liu, N. Hao, Y.-Y. Wang, C. Dou, F. Lin, R. Shen, R. Bura, D. B. Hodge, B. E. Dale, A. J. Ragauskas, B. Yang and J. S. Yuan, *Nat. Commun.*, 2021, **12**, 3912.

11 C. T. Palumbo, E. T. Ouellette, J. Zhu, Y. Román-Leshkov, S. S. Stahl and G. T. Beckham, *Nat. Rev. Chem.*, 2024, **8**, 799–816.

12 M. E. Wolf, A. T. Lalande, B. L. Newman, A. C. Bleem, C. T. Palumbo, G. T. Beckham and L. D. Eltis, *Appl. Environ. Microbiol.*, 2024, **90**, e0215523.

13 M. Park, Y. Chen, M. Thompson, V. T. Benites, B. Fong, C. J. Petzold, E. E. K. Baidoo, J. M. Gladden, P. D. Adams, J. D. Keasling, B. A. Simmons and S. W. Singer, *ChemSusChem*, 2020, **13**, 1–14.

14 A. Rodriguez, D. Salvachúa, R. Katahira, B. A. Black, N. S. Cleveland, M. Reed, H. Smith, E. E. K. Baidoo, J. D. Keasling, B. A. Simmons, G. T. Beckham and J. M. Gladden, *ACS Sustain. Chem. Eng.*, 2017, **5**, 8171–8180.

15 Z. Sun, B. Fridrich, A. de Santi, S. Elangovan and K. Barta, *Chem. Rev.*, 2018, **118**, 614–678.

16 Z. Li, J. Yang and X. J. Loh, *NPG Asia Mater.*, 2016, **8**, e265.

17 I. S. Aldor and J. D. Keasling, *Curr. Opin. Biotechnol.*, 2003, **14**, 475–483.

18 C. Dou, H. Choudhary, Z. Wang, N. R. Baral, M. Mohan, R. A. Aguilar, S. Huang, A. Holiday, D. R. Banatao, S. Singh, C. D. Scown, J. D. Keasling, B. A. Simmons and N. Sun, *One Earth*, 2023, **6**, 1576–1590.

19 R. Sehgal and R. Gupta, *3 Biotech*, 2020, **10**, 549.

20 S. Tomizawa, J.-A. Chuah, K. Matsumoto, Y. Doi and K. Numata, *ACS Sustain. Chem. Eng.*, 2014, **2**, 1106–1113.

21 J. E. Ramírez-Morales, P. Czichowski, V. Besirlioglu, L. Regestein, K. Rabaey, L. M. Blank and M. A. Rosenbaum, *ACS Sustain. Chem. Eng.*, 2021, **9**(31), 10579–10590.

22 Z. Liang, S. Sethupathy, D. Wenqian, H. Jinhao and D. Zhu, *Green Chem.*, 2025, **27**, 5920–5946.

23 E. Arias-Barrau, E. R. Olivera, J. M. Luengo, C. Fernández, B. Galán, J. L. García, E. Díaz and B. Miñambres, *J. Bacteriol.*, 2004, **186**, 5062–5077.

24 N. Y. Abu-Thabit, C. Pérez-Rivero, O. J. Uwaezuoke and N. C. Ngwuluka, *J. Chem. Technol. Biotechnol.*, 2021, **97**(12), 3217–3240.

25 H. R. Ingram, R. J. Martin and J. B. Winterburn, *Appl. Microbiol. Biotechnol.*, 2022, **106**, 6033–6045.

26 J. E. Rodríguez G, S. Brojanigo, M. Basaglia, L. Favaro and S. Casella, *Sci. Total Environ.*, 2021, **794**, 148754.

27 C. Weng, X. Peng and Y. Han, *Biotechnol. Biofuels*, 2021, **14**, 84.

28 H. Choudhary, L. Das, J. G. Pelton, L. Sheps, B. A. Simmons, J. M. Gladden and S. Singh, *Chem.–Eur. J*, 2023, **29**, e202300330.

29 H. Choudhary, M. Mohan, B. A. Simmons, J. M. Gladden and S. Singh, Methods and compositions useful for oxidation of biomass to carboxylic acids using polyoxometalate ionic liquids, *US Patent Application*, **19**, 2025.

30 T. Eng, D. Banerjee, J. Menasalvas, Y. Chen, J. Gin, H. Choudhary, E. Baidoo, J. H. Chen, A. Ekman, R. Kakumanu, Y. L. Diercks, A. Codik, C. Larabell, J. Gladden, B. A. Simmons, J. D. Keasling, C. J. Petzold and A. Mukhopadhyay, *Cell Rep.*, 2023, **42**, 113087.

31 L. Hou, L. Jia, H. M. Morrison, E. L-W Majumder and D. Kumar, *Bioresour. Technol.*, 2021, **342**, 125973.

32 K. L. Burdon, *J. Bacteriol.*, 1946, **52**, 665–678.

33 D. P. Mesquita, A. L. Amaral, C. Leal, A. Oehmen, M. A. M. Reis and E. C. Ferreira, *Anal. Chim. Acta*, 2015, **865**, 8–15.

34 K. Ravi, J. García-Hidalgo, M. F. Gorwa-Grauslund, *et al.*, *Appl. Microbio. Biotechnol.*, 2017, **101**, 5059–5070.

35 X. Jiang, J. A. Ramsay and B. A. Ramsay, *J. Microbiol. Methods*, 2006, **67**, 212–219.

36 M. S. Morlino, R. Serna García, F. Savio, G. Zampieri, T. Morosinotto, L. Treu and S. Campanaro, *Biotechnol. Adv.*, 2023, **69**, 108264.

37 H.-H. Wang, X.-R. Zhou, Q. Liu and G.-Q. Chen, *Appl. Microbiol. Biotechnol.*, 2011, **89**, 1497–1507.

38 D. Salvachúa, T. Rydzak, R. Auwae, A. De Capite, B. A. Black, J. T. Bouvier, N. S. Cleveland, J. R. Elmore, J. D. Huenemann, R. Katahira, W. E. Michener, D. J. Peterson, H. Rohrer, D. R. Vardon, G. T. Beckham and A. M. Guss, *Microb. Biotechnol.*, 2020, **13**, 290–298.

39 M. Li and M. Wilkins, *Bioresour. Technol.*, 2020, **299**, 122676.

40 K. Jawed, V. U. Irorere, R. R. Bommareddy, N. P. Minton and K. Kovács, *Fermentation*, 2022, **8**, 125.